Influence of Heat on Impurity States in an Artificial Semiconductor Atom

A. M. Elabsy

Mansoura University, Faculty of Science Department of Physics, Mansoura, Egypt.

The present work investigates the influence of heat on the donor impurity states in a man-made artificial semiconductor atom (ASA) based on a nano-meter scale, the so-called quantum dot (QD). An on-center donor impurity is considered. The investigated nanostructure is composed of a GaAs semiconductor as the potential well material of the ASA while an $Al_xGa_{1-x}As$ semiconductor as the potential barrier material of the artificial atom. Different heat dependent effective masses and different heat dependent dielectric constants are used for the two semiconductors constitute the ASA. The lowest energy and the binding energy of the ground state are calculated. The calculations have shown that the lowest electron energy decreases by increasing the ASA radius. For very large radii the lowest energies corresponding to different aluminum contents approach a certain value which is the bulk limit. At a constant ASA radius the lowest energy increases as a function of temperature. A pronounced deviation is obtained when the calculations of the present work are compared with those of Montenegro and Merchancano [18] in which the effects of heat and mismatches for both effective masses and dielectric constants were neglected. It is found that decreasing the temperature and shrinking the radius of the ASA lead to more binding of the donor electron. Increasing the aluminum concentration also enhances the donor electron binding energy. Therefore the electron ground state energy and its associated binding energy are both mainly functions of temperature, ASA radius, and aluminum content.

Introduction

Scales of about 10 nanometer (nm) [6]. The less of dimensions in these new systems produces a new quantum physics of semiconductors with discrete energy spectrum. This physical phenomena is created by confining potentials in one, such as quantum well (QW) systems, or two, such as quantum well wire (QWW) systems, and three directions, such as artificial atoms or quantum dot (QD) systems [7]. These man-made nanostructures have potential applications in high-speed field-effect transistors, solar cells, and high-efficiency lasers and detectors [8].

Impurities play an essential role in governing both the transport and optical properties in semiconductors. Spectroscopy of imperfections (donors and acceptors) in semiconductors has showed small binding energy of electrons (holes) compared to the intrinsic energy gap of the host. The wave functions characterizing the energy levels of the imperfection are extended over many lattice spacings [9].

In quantum heterostructures the impurity wavefunction is severely affected by the barrier potential. Consequently, the binding energy depends not only on the width of the well but also on the precise location of the impurity [10].

Due to the rapid progress in fabrication and experimental investigations [6,11-17] of artificial atoms (QD's), theoretical techniques are developed to study the carriers confinement in these systems. The ground states energy and the binding energy of shallow hydrogenic impurities in artificial atoms or spherical GaAs(Ga,Al)As QD's as functions of the radius of the atom or dot and for both infinite and finite confining potentials were calculated by Montenegro and Merchancano [18]. They found that the impurity binding energy is increased as the dot radius decreases for an infinite well whereas it reaches a peak value and then diminishes to a limiting value for a finite potential. The binding energies of hydrogenic donor for both infinite and finite GaAs(Ga,Al)As spherical QD’s as a function of the donor position for different radii and also the density of impurity states as a function of the donor binding energy were evaluated by Montenegro et al. [19]. Zhu and Chen [20] computed variationally the ground and excited states and binding energies of an off center donor in GaAs-Ga1-xAlxAs spherical QD's with a finite barrier height. Their results demonstrated the quantum size effect. The effects of spatially dependent dielectric screening of an impurity ion caused by the valence electrons of GaAs and the dielectric mismatch between the barrier and the well materials were addressed for both infinite [21,22] and finite [21-23] potential wells. The effect

of nonparabolicity of the GaAs conduction band on the binding energy of a hydrogenic donor in a GaAs/AlxGa1-xAs QD was considered by Elabsy and Csavinszky [23,24]. Riberio and Latgé [25] reported the dependence of the donor binding energy and density of impurity states of a hydrogenic impurity in a QD on the volume of the dot and on the impurity position. They compared the donor binding energies for cubic and spherical QD's, with same volume, and found that the values are very close. Tulkki and Heinämäki [26] computed the energy levels for an In1-xGaxAs/GaAs QD by including the strain interaction and the band edge confinement in the Luttinger-Kohn Hamiltonian. Their calculations provided indirect evidence of screened Coulomb interaction addressed to slow carrier relaxation. Recently Cusak et al. [27] have evaluated the electronic structure of InAs/GaAs QD's by taking into account the microscopic details of the strain and valence-band mixing and the change in effective masses due to strain.

1. In all the above calculations, the influence of heat on the energy states and binding energies of impurities confined to ASA's are neglected. Therefore, this paper follows a variational approach to investigate the influence of heat on the binding energy of an on-center donor impurity confined to a nanostructural $Al_xGa_{1-x}As/GaAs/Al_xGa_{1-x}As$ artificial atom (ASA). The units used are the atomic units in which $e=\hbar=m_0=1$, the unit of energy is Hartree, and the unit of length is Bohr.

2. Theory

The Hamiltonian for an on-center donor electron in a nanostructural $Al_xGa_{1-x}As$ /GaAs/ $Al_xGa_{1-x}As$ artificial atom of radius R is given by

$$H(r,T)=K(r,T)+V(r,T)+V_b(r,T) \qquad ...(1a)$$

where

$$K(r,T) = -\frac{1}{2m^*_{1,2}(T)}\nabla^2, \qquad \ldots(1b)$$

$$V(r,T) = -\frac{1}{\varepsilon_{1,2}(T)\,r}, \qquad (1c)$$

$$V_b(T)=\begin{cases} 0; & r \le R, \\ V_0(T); & r \ge R. \end{cases} \qquad (1d)$$

In the above equation (1d), $V_0(T)$ is the height of the confining potential. It is obtained from the temperature dependent band-gap discontinuity $E_g(x, T)$, given in eV, [28,29] as

$$V_0(T) = 0.60\Delta E_g(x,T) \qquad (1e)$$

In equation (1e), $\Delta E_g(x, T) = x\,(A - B\,T)$; with A = 1.247 eV and B = $1.15\text{x}10^{-4}$ eV/K for an aluminum mole fraction of x < 0.45. $m^*_{1,2}(T)$ and $\varepsilon_{1,2}(T)$ [28,29] are the heat dependent effective-masses and dielectric constants of the artificial atom materials, respectively. T is the absolute temperature given in Kelvin, which lies in the range from 0 K to 900 K [30]. The subscript 1 refers to the potential well material, GaAs, whereas the subscript 2 refers to the potential barrier, $Al_xGa_{1-x}As$, material.

The variational ground state wavefunction for the given confining potential is chosen [18,22-24] as

$$\Psi(r,T) = \begin{cases} \Phi_1(r,T); & r \le R, \\ \Phi_2(r,T); & r \ge R. \end{cases} \qquad \ldots(2a)$$

where

$$\Phi_1(r,T) = \frac{\Gamma}{r}\sin[\zeta(T)r]\exp(-\lambda r), \qquad \ldots(2b)$$

and

$$\Phi_2(r,T) = \frac{\Gamma}{r}\sin[\zeta(T)R]\exp\{\kappa(T)[R-r]-\lambda r\}. \qquad \ldots(2c)$$

In the above two expressions, Γ is a normalization constant, λ is a variational parameter, $\zeta(T) = [2\,m^*_1(T)\,E_0(T)]^{1/2}$, and $\kappa(T)=\{2\,m^*_2(T)\,[V_0(T)-E_0(T)]\}^{1/2}$.

$E_0(T)$ is the lowest energy state in the absence of the donor impurity and is obtained by imposing the matching condition at the interface (r = R) that $(1/m^*_i)\;\partial\Phi_{0i}(r,T)/\partial r$, where $\Phi_{0i}(r,T)$ is the solution of the Hamiltonian by neglecting the impurity potential i.e. by replacing λ = 0 in equations (2b) and (2c). One obtains a transcendental equation in the form

$$\tan[\zeta(T)R] = -\frac{\mu(T)\zeta(T)}{\kappa(T)+[1-\mu(T)]/R} \qquad \ldots(3)$$

where $\mu(T) = m^*_2(T)/m^*_1(T)$ is the ratio of effective masses. Solving equation (3) numerically on gets $E_0(T)$. The temperature dependent variational binding energy E of a donor electron is given by

$$E = E_0(T) - H_{min}(r,T) \qquad \ldots(4)$$

where $H_{min}(r,T)$ is determined by minimizing the total expectation energy, $\langle \Psi | H | \Psi \rangle$ with respect to the variational parameter λ.

3. Discussion

Figure (1) exhibits the relation between the heat dependent lowest energy, $E_0(T)$, in meV and the ASA radius, R, in nm units. The calculations are performed for three aluminum concentrations, x = 0.15 and 0.30, and 0.45 at a constant temperature, T, of 300 K. It is seen from the figure that the curves decrease with increasing the ASA radius, R. The deviations between the curves decrease by increasing the ASA radius. It is also seen from Fig. (1) that, the values of lowest energy for x = 0.30 based on the model of Montenegro and Merchancano [18], which considers equal effective masses and equal dielectric constants for both materials and energy gap difference at mixed temperatures, deviate from the present calculations. This discrepancy is of about 7% for an atom radius of 2.7 nm at 300 K and is about 6% at 4 K. If the atom radius becomes very large the energy values approach each other and coincide in the bulk limit.

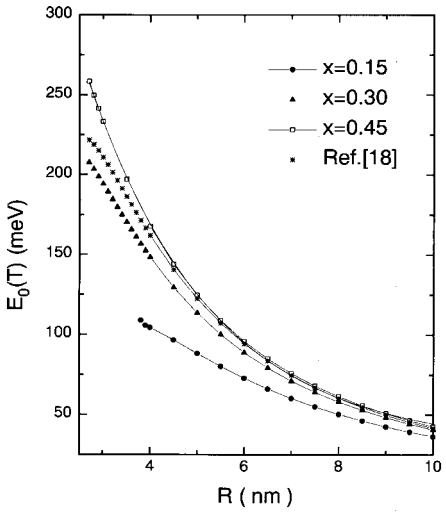

Fig.(1): Heat dependence lowest energy, $E_0(T)$, in meV versus the ASA radius, R, in nm for aluminum contents x = 0.15, 0.30, and 0.45. The (***) refer to the calculations based on Ref.[18] for x = 0.30.

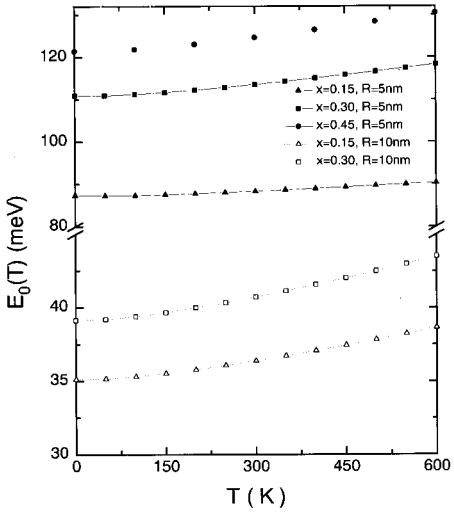

Fig.(2): The lowest energy, $E_0(T)$, in meV as a function of temperature, T, in Kelvin for two ASA radii (R = 5 nm and 10 nm) at three aluminum concentrations (x = 0.15, 0.30, and 0.45)

Fig. (2) shows the variation of the ground state energy, E_0 (T), in meV as a function of temperature for three aluminum contents x = 0.15, 0.30, and 0.45 at two fixed ASA radii, R = 5 nm and 10 nm. It is seen from the figure that the energies increase for all cases with increasing temperature. In comparison with the calculations based on Ref .[18] for x = 0.30, one finds that the values of E_0 based on Ref .[18] are 122.38 meV for R = 5 nm and 41.65 meV for R = 10 nm. The present calculations give 110.93 meV and 113.53 meV for R = 5 nm, and 39.14 meV and 40.72 meV for R = 10 nm at T = 4 K and 300 K, respectively. These discrepancies manifest their behavior in the mixed temperature and equal values of parameters for the two materials constitute the ASA. The values of the parameters are different and vary with temperatures as shown in Table (I).

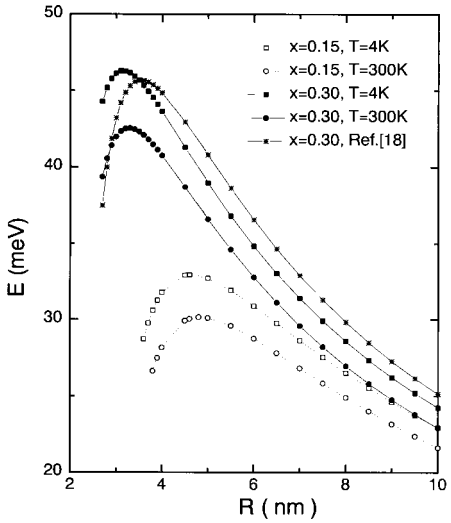

Fig. (3): Heat dependence binding energy, E, in meV, versus the artificial atom radius R, in nm for two values of temperature (T = 4 K and 300 K) and at two aluminum contents (x = 0.15 and 0.30). The (***) denote to the calculations based on Ref.[18] for x = 0.30.

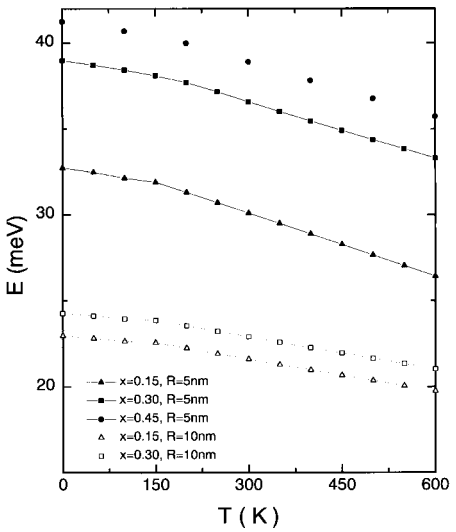

Fig. (4): The lowest binding energy, E, in meV, as a function of temperature at ASA radii of 5 nm and 10 nm for three aluminum concentrations (x = 0.15, 0.30, and 0.45).

Fig. (3) shows the variation of the electron binding energy, E (meV), associated with the ground state versus the ASA radius, R (nm) for two different values of temperature, T = 4 K and 300 K, and at two aluminum concentrations x = 0.15 and 0.30. It is also seen from Fig. (3) that, at a fixed

temperature the binding energy increases until it reaches a maximum value at a specific radius and then decreases as R increases. For very large radii all curves approach the bulk limit value of GaAs. These behaviors are the same as of Ref. [18]. For smaller radii, the wave function spills to the potential barrier material leading to less probability of finding the electron inside the artificial atom, which in turn leads to small binding energy. One can also see that the donor's binding energy depends on the aluminum content in the $Al_xGa_{1-x}As$ material. Increasing the x value of aluminum enhances the binding energy. This increment in energy is due to the fact that the excess of aluminum content expands the energy gap between the two materials which in turn increases the potential barrier height leading to more binding of the electron. From figure (3) one finds that there is a large discrepancy between the present work and that based on Ref.[18]. In Ref.[18], they used the same values for both masses and dielectric constants at very low temperatures ($m_1^* = m_2^* = 0.0665$ and $\varepsilon_1 = \varepsilon_2 = 12.58$) while the energy gap difference is taken at room temperature. These values vary with temperature as shown in Table (I). The percentage energy difference between the binding energies at temperatures of 4 K and 300 K for x=0.30 is about 13% at an atom radius of 2.7 nm, while it decreases with increasing the atom radius.

Table (I)
The heat dependence of material parameters for the two materials constitute the ASA. The two subscripts 1 and 2 refer to the GaAs and $Al_xGa_{1-x}As$, respectively.

T(K)	$m_1^*(T)$	$\varepsilon_1(T)$	X = 0.15		X = 0.30		X = 0.45	
			$m_2^*(T)$	$\varepsilon_2(T)$	$m_2^*(T)$	$\varepsilon_2(T)$	$m_2^*(T)$	$\varepsilon_2(T)$
0	0.066998	12.65	0.079448	12.18	0.091898	11.71	0.104348	11.25
100	0.066305	12.77	0.078755	12.30	0.091205	11.83	0.103655	11.37
200	0.064908	12.91	0.077358	12.45	0.089808	11.89	0.102258	11.51
300	0.063221	13.18	0.075671	12.71	0.088121	12.24	0.100571	11.78
400	0.061382	13.45	0.073832	12.98	0.086282	12.52	0.098732	12.05
500	0.059451	13.73	0.071901	13.26	0.084351	12.79	0.096801	12.32
600	0.057459	14.01	0.069909	13.54	0.082359	13.08	0.094809	12.61

Fig. (4) displays the dependence of the lowest donor electron binding energy, E (meV), for three different mole fractions of aluminum (x = 0.15, 0.30, and 0.45) at two ASA radii (R = 5 nm and 10 nm). It is seen from Fig. (4) that, the lowest electron binding energies for fixed values of R are enhanced by lowering the temperature, T. This finding is due to the fact that, the position

probability of finding the electron in the semiconductor atom is larger at a low temperature than that corresponding to a high temperature. It is also seen from Fig. (4) that, for fixed values of x, the binding energies decrease by increasing the atom radius. One finds that the discrepancy in energy for different x values diminishes with increasing R. As a matter of fact, the higher mole fraction of aluminum in the potential barrier, $Al_xGa_{1-x}As$, material raises the height of the potential barrier which leads to more confinement of the donor electron inside the artificial atom, and consequently greater binding energy. Furthermore, the main feature of the curves shown in Fig. (4) is that the binding energy decreases by increasing temperature.

4. Conclusion

It can be concluded that the ground state binding energy of an electron associated with a donor impurity localized in artificial semiconductor atoms (ASA's) based on a nano-meter scale is more affected by heat. The binding energy of the donor electron is enhanced not only at a low temperature but also by decreasing the artificial atom radius. Increasing the aluminum mole fraction in the barrier material of the artificial atom also increases the donor electron binding energy. In the calculations of the carriers binding energies for impurities immersed in ASA's effects of mismatches of the parameters constitute the ASA have to be considered and must be taken at the same temperature.

References

1. Y. Cho, J. Appl. Phys. **42**, 2074(1971).
2. E. H. C. Parker, The Technology and Physics of Molecular Beam Epitaxy (Plenum, New York, 1985).
3. J. Cibert, P. M. Petroff, G. J. Dolan, A. C. Gossard, and J. J. English, Appl. Phys. Lett. **49**, 1275(1986).
4. H. M. Manasevit, J. Electrochem. Sec. **118**, 647(1971).
5. R. D. Dupus and P. D. Dapkus, in 7th International Symposium on GaAs and Related Compounds, St Louis, 1978, C. M. Wolfe, Ed. (Institute Of Physics, London 1979) pp.1-9.
6. Y. Arakawa, Solid-State Electronics **37**,523, (1994).
7. G. Kirczenow, Phys. Rev. B**46**, 1439 (1992).
8. N. J. Shah and -S. Pei, AT&T Tech. J. **68**, 5(1989).
9. A. K. Ramdas and S. Rodriguez, Rep. Prog. Phys. **44**, 1997(1981).
10. G. Bastard, Phys. Rev. B**24**, 4714(1981).
11. H. Drexler. D. Leonard, W. Hansen, J. P. Kotthaus, and P. M. Petroff, Phys. Rev. Lett. **73**, 2252 (1994).

12. G. M. Ribeiro, D. Leonard, and P. M. Petroff, Appl. Phys. Lett. **66**, 1767(1995).
13. D. Heitmann, Phyica B**212**, 201(1995).
14. R. J. Haug, R. H. Blick, and T. Schmidt, Phyica B**212**, 207(1995).
15. J.-Y. Marzin, J.-M. Gerard, A. Izrael, D. Barrier, and G. Bastard, Phys. Rev. Lett.**73**, 716 (1994).
16. J. M. Moison, F. Hauzay, F. Barthe, L. Leprince, E. André, and O. Vatel, Appl. Phys. Lett. **64**, 196(1994).
17. D. Leonard, M. Krishnamurthy, C. M. Reaves, S. P. Denbaars, and P. M. Petroff, Appl. Phys. Lett. **63**, 3203(1993).
18. N. P. Montenegro and S. T. P. Merchancano, Phys. Rev. B**46**, 9780 (1992).
19. N. P. Montenegro, S. T. P. Merchancano, and A. Latgé, J. Appl. Phys. **74**, 7624(1993).
20 .J. L. Zhu and X. Chen., Phys. Rev. B**50**, 4497(1994).
21. Z. Y. Deng, J. K. Guo, and T. R. Lai, Phys. Rev. B**50**, 5736(1994).
22. A. M. Elabsy and P. Csavinszky, Croat. Chem. Acta **86**, 309(1995).
23. A. M. Elabsy and P. Csavinszky, Int. J. Quant. Chem.: Quant. Chem. Symp. **30**, 1719(1996).
24. A. M. Elabsy and P. Csavinszky, J. Math Chem. **16**, 309 (1994).
25. F. J. Riberio and A. Latgé, Phys. Rev. B **50**, 4913(1994).
26. Tulkki and A. Heinämäki, Phys. Rev. B52, 8239(1995).
27. M. A. Cusak, P. R. Bridden, and M. Jarros, Phys. Rev. B54, R2300(1996).
28. J. Batey and S. L. Wright, J. Appl. Phys. **59**, 200(1986).
29. A. M. Elabsy, J. Phys.: Condens. Matter **6**, 10025(1994).
30. S. M. Sze, Physics of Semiconductor Devices, 2nd edit. (john Wiley & Sons, Inc., New York, 1981), p15.